



Neurofascin (NFASC) gene mutation causes autosomal recessive ataxia with demyelinating neuropathy

Edoardo Monfrini^{a,b}, Letizia Straniero^{c,d}, Sara Bonato^{a,b}, Giacomo Monzio Compagnoni^{a,b},
 Andreina Bordoni^{a,b}, Robertino Dilella^e, Paola Rinchetti^{a,b}, Rosamaria Silipigni^f, Dario Ronchi^{a,b},
 Stefania Corti^{a,b}, Giacomo P. Comi^{a,b}, Nereo Bresolin^{a,b}, Stefano Duga^{c,d}, Alessio Di Fonzo^{a,b,*}

^a Foundation IRCCS Ca' Granda Ospedale Maggiore Policlinico, Neurology Unit, Milan, Italy

^b Dino Ferrari Center, Neuroscience Section, Department of Pathophysiology and Transplantation, University of Milan, Milan, Italy

^c Department of Biomedical Sciences, Humanitas University, Pieve Emanuele, Milan, Italy

^d Humanitas Clinical and Research Center, Rozzano, Milan, Italy

^e Fondazione IRCCS Ca' Granda Ospedale Maggiore Policlinico, Neurofisiopatologia Pediatrica, UOC Neurofisiopatologia, Milan, Italy

^f Fondazione IRCCS Ca' Granda Ospedale Maggiore Policlinico, Laboratory of Medical Genetics, Milan, Italy

ARTICLE INFO

Keywords:

Neurofascin
 NFASC
 Hereditary Ataxia
 Neuropathy
 Nodopathy

ABSTRACT

Introduction: Neurofascin, encoded by *NFASC*, is a transmembrane protein that plays an essential role in nervous system development and node of Ranvier function. *Anti*-Neurofascin autoantibodies cause a specific type of chronic inflammatory demyelinating polyneuropathy (CIDP) often characterized by cerebellar ataxia and tremor. Recently, homozygous *NFASC* mutations were recently associated with a neurodevelopmental disorder in two families.

Methods: A combined approach of linkage analysis and whole-exome sequencing was performed to find the genetic cause of early-onset cerebellar ataxia and demyelinating neuropathy in two siblings from a consanguineous Italian family. Functional studies were conducted on neurons from induced pluripotent stem cells (iPSCs) generated from the patients.

Results: Genetic analysis revealed a homozygous p.V1122E mutation in *NFASC*. This mutation, affecting a highly conserved hydrophobic transmembrane domain residue, led to significant loss of Neurofascin protein in the iPSC-derived neurons of affected siblings.

Conclusions: The identification of *NFASC* mutations paves the way for genetic research in the developing field of nodopathies, an emerging pathological entity involving the nodes of Ranvier, which are associated for the first time with a hereditary ataxia syndrome with neuropathy.

1. Introduction

Neurofascin, a member of the L1 immunoglobulin cell adhesion molecule family (L1CAM) family, is a transmembrane protein, encoded by *NFASC*, an evolutionarily conserved gene located on chromosome 1q32, and ubiquitously expressed in human tissues [1]. Neurofascin protein is abundant in the adult central nervous system, especially in the cerebellum and peripheral nerves [2,3]. Moreover, Neurofascin plays a pivotal role in the development and function of the axon initial segment (AIS) and the nodes of Ranvier [4,5]. Both the AIS and node of Ranvier contain a high density of sodium voltage-gated channels, necessary for action potential generation and propagation, which are clustered by interactions with several cytoskeletal and scaffolding

proteins, including Neurofascin. Another recognized role of Neurofascin is to connecting the extracellular matrix and glial cells (Schwann cells and oligodendroglia) with the intracellular skeleton of neurons [6–8].

NFASC transcripts undergo extensive alternative splicing and protein isoforms are differentially expressed in the central and peripheral nervous systems in a developmental- and cell type-specific manner. In the adult mouse, Neurofascin has two principal isoforms: the neuronal isoform (138 kDa), known as NF186, and the glial isoform (133 kDa), known as NF155. These proteins are highly glycosylated with observed molecular weights on Western blot of 186 kDa and 155 kDa respectively [9,10]. Similarly, adult human nervous tissues have two principal Neurofascin isoforms with molecular weights of 186 kDa and 150 kDa.

Here, we describe two affected siblings from a consanguineous

* Corresponding author. Neurology Unit, IRCCS Foundation Ca' Granda Ospedale Maggiore Policlinico, Via Francesco Sforza 35, 20122, Milan, Italy.

E-mail address: alessio.difonzo@policlinico.mi.it (A. Di Fonzo).

Italian family presenting with infantile-onset ataxia and mild demyelinating polyneuropathy who carry a homozygous *NFASC* missense mutation.

2. Materials and methods

2.1. Clinical data

Patients were subjected to general and neurological examination by an ataxia-experienced neurologist. Both affected individuals underwent brain MRI and neurophysiological studies. Blood samples were collected. The Ethics Committee of the IRCCS Foundation Ca' Granda Ospedale Maggiore Policlinico (Milan, Italy) approved the study. Written informed consent was obtained from all involved subjects.

2.2. Genetic analysis

Genomic DNA was extracted from peripheral venous blood from all family members by standard salting-out procedures. All subjects were genotyped using the Infinium OmniExpressExome-8 v1.3 BeadChip array, which includes a total of 958,497 markers, with a mean spacing of 3.03 kb. A multipoint parametric linkage analysis was performed using Allegro software to identify chromosomal loci compatible with recessive inheritance (Used map: Illumina 650 k HumanHap v3 deCODE; Inheritance: Recessive; Penetrance: 99%; Scoring function: HOMOZ and MNAllele).

Individual II.1 (see Fig. 1) was analyzed by whole exome sequencing (WES) starting from 50 ng of genomic DNA using the Nextera Rapid Capture Exome Library kit (Illumina, San Diego, CA, USA) and the Illumina NextSeq500 platform (Illumina) according to the manufacturer instructions. Reads were aligned against the human reference genome (hg19) using BWA [11]. Variant calling was performed with GATK [12] and variant annotation with ANNOVAR (<http://annovar.openbioinformatics.org/en/latest/>). The candidate variants and their

segregation in the family were validated by Sanger sequencing. Primers used for PCR amplification and Sanger sequencing of *NFASC* and *NSMCE4A* are listed in [Supplementary Table 1](#).

Array comparative genomic hybridization (array-CGH) was performed using an Agilent SurePrint G3 human 4 × 180 K kit. Data were analyzed using CytoGenomics 3.0 (Agilent Technologies, Santa Clara, CA, USA). Aberrations were considered when the involved genomic region was covered by at least three adjacent probes and all arrays showed a derivative log ratio (DLR) spread < 0.2. Genomic coordinates were based on the 37 build (February 2009) of the Human Genome Reference Consortium (GRCh37/hg19).

2.3. Cell cultures

Skin punch biopsies were obtained from the ventral part of the left forearm of both affected siblings. Fibroblasts were cultured in DMEM high glucose supplemented with 15% fetal bovine serum (Euroclone, Milan, Italy), 1% penicillin/streptomycin (Sigma-Aldrich, Saint Louis, MO, USA), and 1% of amphotericin B (Sigma-Aldrich).

Fibroblasts were reprogrammed to induced pluripotent stem cells (iPSCs) using the CytoTune-iPS 2.0 Sendai Reprogramming Kit (Life Technologies, Carlsbad, CA, USA). Clones with an iPSC-like morphology underwent karyotype analysis, and those carrying a normal karyotype were used for differentiation ([Supplementary Fig. 1A](#)). iPSCs were differentiated to fully mature neurons using the method described by Zhang et al. [13] ([Supplementary Table 2](#) and [Supplementary Figs. 1B–C](#)).

2.4. Immunocytofluorescence

Immunocytofluorescence studies were performed according to standard protocols. The iPSCs and neurons were stained with primary antibodies detecting Sox 2 (ab15830, Abcam, Cambridge, UK), Neurofascin (ab31457, Abcam), β -tubulin III (T8660, Sigma-Aldrich),

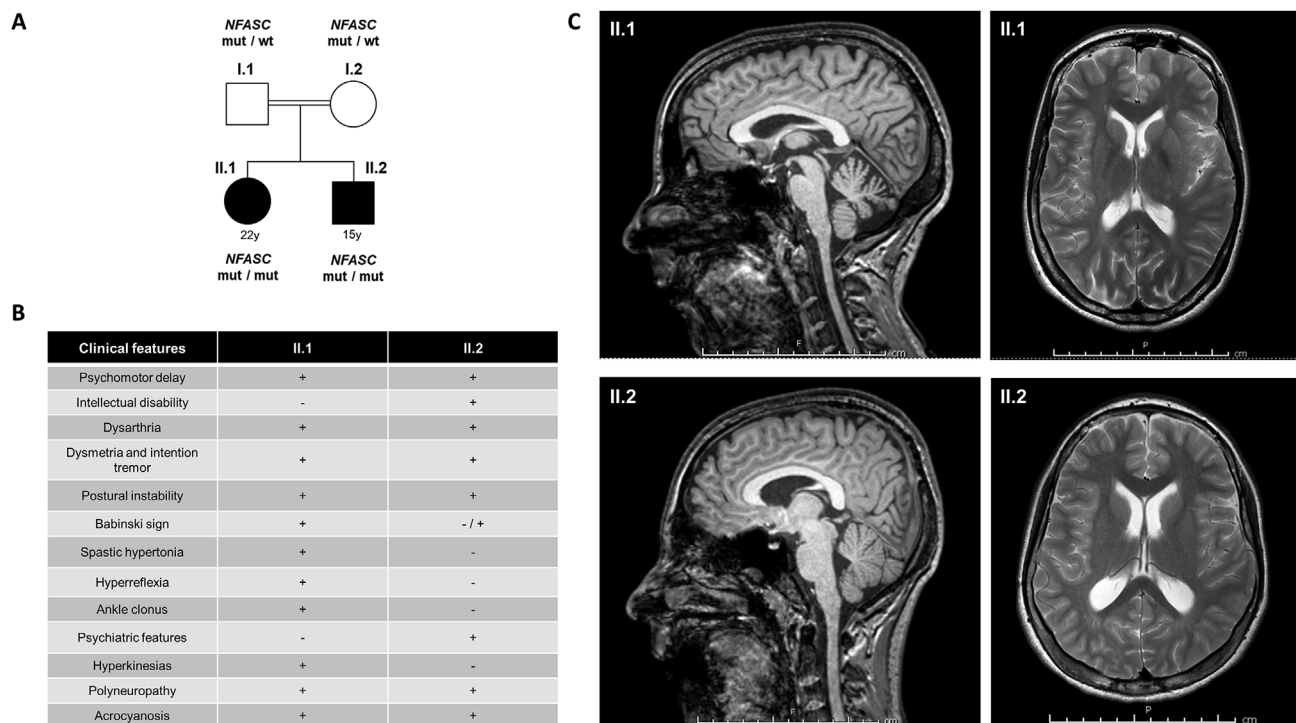


Fig. 1. Family pedigree, clinical features, and brain MRI. A) Pedigree of the family under study. Black symbols denote affected individuals. B) Clinical characteristics of subjects II.1 and II.2 ("+" = presence, "-" = absence, "- / +" = intermediate features). C) Brain MRI of subjects II.1 and II.2 (sagittal T1 on the left and axial T2 on the right) performed at 22 and 15 years of age respectively, showing mild atrophy of the cerebellar vermis in subject II.1 and a mild diffuse T2 hyperintensity of white matter, probably due to hypomyelination, in both probands.

and MAP2 (M9942, Sigma-Aldrich). Alexa Fluor 488 and Alexa Fluor 594 were used as secondary antibodies (Life Technologies). Images were acquired using a Leica SP5 confocal microscope system (Leica Biosystems, Wetzlar, Germany). ImageJ software was used to assess fluorescence intensity [14].

2.5. Protein blotting and sub-cellular fractionation

Whole-protein lysates were obtained by standard methods. Subcellular fractionation was performed using the Subcellular Protein Fractionation Kit for Cultured Cells (Thermo Fisher Scientific, Waltham, MA, USA) according to the manufacturer's instructions. Fraction-specific markers were evaluated by Western blot (α -tubulin for cytoplasm; COX-IV for cell and mitochondrial membranes). Western blot analyses were performed in triplicate according to standard procedures using the following primary antibodies: Neurofascin (ab31457, Abcam); α -tubulin (MCA3560Z, AbD Serotec, Kidlington, UK), COX-IV (A21348, Life Technologies), actin (A2066, Sigma-Aldrich). The anti-Neurofascin antibody is directed against the intracellular domain of the protein and detects different protein isoforms in human brain (e.g. NF186 and NF155) (Fig. 4A).

2.6. Data availability

The data that support the findings of this study are available from the corresponding author, upon reasonable request.

3. Results

3.1. Clinical features

The family originated from an isolated valley of Northern Italy. The parents (subjects I.1 and I.2) were first cousins (Fig. 1A). The two affected siblings were 22 (subject II.1) and 15 (subject II.2) years old at first examination. The probands presented an early psychomotor delay and the younger brother exhibited a mild intellectual disability. They started to walk at 3 years of age with an unsteady wide-based ataxic gait. Cerebellar dysarthria, intention tremor, dysmetria, pursuit saccadization, and dysidiadochokinesia were also observed. Eye closing did not worsen ataxic features, suggesting a primary cerebellar involvement.

From the age of 11 years, subject II.1 developed progressive spastic hypertonia of the limbs with hyperreflexia, lower limbs intra-rotation, ankle clonus, and bilateral Babinski sign. A therapeutic challenge with baclofen (*per os* and intrathecal) was not successful. At 16 years of age, she started to use a wheelchair outside the house and required bilateral support for standing. In addition, remarkable sleepiness in the morning appeared, which responded well to modafinil (50 mg die). Mild dysphagia was demonstrated at 18 years of age. At 24 years old, she developed involuntary sub-continuous non-rhythmic myoclonic jerks in the proximal upper limbs, which disappeared during sleep and were aggravated by anxiety and emotions.

Subject II.2 did not develop hypertonia of the limbs or hyperreflexia. From the age of 12 years, he had episodes of aggression and intense anxiety, associated with reality detachment and perseverations. Partial remission of these episodes was achieved with low doses of arripirazole and paroxetine.

Brain MRI showed mild atrophy of the cerebellum in the older sibling and a mild diffuse T2 hyperintensity of periventricular white matter in both probands, probably due to brain hypomyelination (Fig. 1C). Electroencephalography (EEG) showed bilateral fronto-temporal slowing in both probands. The involuntary movements of subject II.1 were not associated with EEG abnormalities. Motor evoked potentials (MEPs) showed a marked slowing of the central conduction velocity in both the upper and lower limbs. Somatosensory evoked potentials (SEPs) showed a mild to moderate slowing of the central

conduction velocity. Pattern shift visual evoked potentials (VEPs) were within normal limits in II.2, but they could not be reliably assessed in II.1 because of artefacts due to the continuous involuntary movements. However, flash VEPs could be assessed and their latency appeared to be mildly increased. Nerve conduction studies showed a mild length-dependent demyelinating sensory-motor peripheral neuropathy, which was more evident in II.2 than in II.1 (Supplementary Table 3). The sensory contribution to ataxia was considered to be of minor importance considering that the neuropathy was mild and not evident at the neurological examination, the central and peripheral sensory tracts and fibers were less involved than the motor counterparts, and closing the eyes did not worsen the ataxic features.

Muscle biopsies performed on both siblings were unremarkable. Ocular fundus examinations were normal. No cardiological abnormalities were found. Standard blood tests were normal.

3.2. Genetic analysis

SCA1, *SCA2*, *SCA3*, *SCA6*, *SCA8*, *SCA10*, *SCA12*, *SCA17*, *DRPLA*, and Friedreich's ataxia pathological expansions were ruled out. Screening for mutations in *SPG4*, *SPG7*, *SPG11*, *SPG15*, *SPG35*, *SETX*, *ARSACS*, *SCA28*, and *PLA2G6* was negative. Karyotype and array-CGH were normal. The family pedigree and consanguinity of the parents strongly suggested an autosomal recessive pattern of inheritance, with a homozygous mutation being suspected as the cause of the disease.

Linkage analysis identified two haploidentical homozygous regions in the two affected individuals on chromosomes 1 and 10 (Fig. 2A). Flanking markers of the homozygous regions were rs4951272-rs11572795 for chromosome 1 and rs2765471-rs716909 for chromosome 10. A single gene known to be involved in genetic ataxias was present in the linked regions, *SYT14* located on chromosome 1 and coding for synaptotagmin XIV. However, no variants were found in the patients by Sanger sequencing of *SYT14* exons and intron-exon boundaries.

WES was performed on subject II.1, obtaining a mean coverage depth of 76.1 with 92% of the bases of the target region having $\geq 20\times$ coverage (97.5% with coverage $\geq 10\times$). No pathogenic mutations were found in known disease genes for hereditary ataxias, spastic paraplegias, or neuropathies. A filtering analysis for rare (allele frequency $< 1\%$) variants with protein impact (missense, nonsense, frameshift, inframe ins/del, nonstop, misstart, splice disruptive) was performed in the homozygous linkage regions. Only two novel homozygous variants were identified: c.3365T > A, p.V1122E in *NFASC* (NM_001005388), and c.754–5_754-4delTT in *NSMCE4A* (NM_001167865, coding for NSMCE4a protein). The mutations were confirmed to be homozygous in subjects II.1 and II.2 and heterozygous in both parents by Sanger sequencing (Fig. 2B and Supplementary Fig. 2A).

The *NSMCE4A* c.754–5_754-4delTT is a novel variant near the splicing acceptor site of exon 6. The deleted nucleotides are not conserved in mammals and, in contrast to *NFASC*, *NSMCE4A* is not preferentially expressed in nerve tissue, but rather in the bladder, colon, uterus, and prostate. Moreover, Mutation Taster and CADD did not predict this variant to be deleterious. *NSMCE4A* is tolerant to loss of function mutations (probability of being loss-of-function intolerant [pLI] 0.09, ExAC Browser) in contrast to the extremely intolerant pLI value of 1.0 for *NFASC*. However, analysis of the patients' cDNA showed a higher expression of an alternative spliced transcript due to skipping exon 6 (XR_001747116.1) in addition to the normal transcript (NM_001167865) (Supplementary Figs. 2B–C), and a possible contribution to the disease cannot be ruled out.

The p.V1122E *NFASC* mutation is a novel variant absent from public databases. The valine at position 1122 is highly conserved in orthologous proteins and lies in the unique Neurofascin transmembrane domain, which is present in all protein isoforms. Substitution with a hydrophilic glutamic acid (Fig. 2C) is expected to affect the

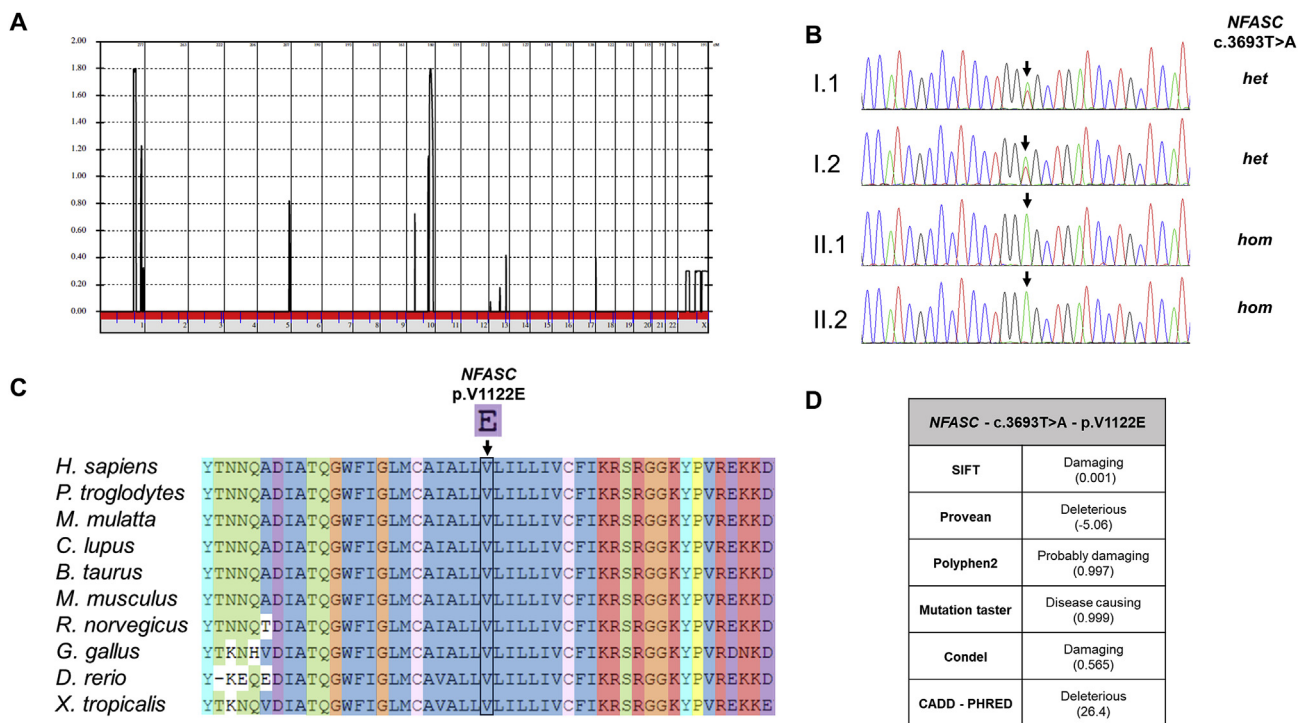


Fig. 2. Genetic and bioinformatic analysis. A) Linkage analysis plot displaying LODscore values at different chromosomal regions (multipoint parametric analysis, scoring function: HOMOZ). Two peaks on chromosomes 1 and 10 indicate haploidentical homozygous regions in the two affected siblings. B) Electropherograms of the *NFASC* c.3693 T > A homozygous mutation in the probands (II.1 and II.2) and the heterozygous mutation in their parents (I.1 and I.2). C) Alignment of Neurofascin protein homologs showing conservation of the amino acid mutated in this family (Valine 1122). The colors represent those used in the ClustalW multiple sequence alignment program [27]. Each residue in the alignment is assigned a color if the amino acid profile at that position meets the minimum criteria specific for the residue type (blue = hydrophobic, magenta = positively charged, red = negatively charged, green = polar, cyan = aromatic, pink = cysteines, orange = glycines, yellow = prolines). D) Assessment of the deleterious impact of the *NFASC* p.V1122E variant by in silico prediction tools SIFT, Provean, Polyphen2, Mutation Taster, Condel, and CADD. (For interpretation of the references to color in this figure legend, the reader is referred to the Web version of this article.)

transmembrane domain leading to impaired Neurofascin stability and function. Pathogenicity prediction tools SIFT, Provean, Polyphen2, Condel, Mutation Taster, and CADD were used to assess the impact of the identified variant. The *NFASC* p.V1122E mutation was predicted by all prediction tools to be deleterious (Fig. 2D). The cDNA analysis did not show a reduced amount of *NFASC* transcript in patients compared to controls.

Therefore, *NFASC* was prioritized as the candidate etiological gene in this family. To assess this hypothesis, functional studies were performed on iPSC-derived neurons.

3.3. Cellular and protein studies

Fibroblasts from the two affected siblings and three healthy controls were cultured from skin biopsies. Because Neurofascin is not expressed in fibroblasts, they were reprogrammed to iPSCs and then differentiated into mature neurons. Immunocytofluorescence (ICF), performed at 50 days in vitro (DIV) showed a discrete Neurofascin distribution within controls neuron somata and several smaller spots of staining in neuronal somata and extensions (Fig. 3A–B). Neurofascin immunofluorescence was significantly reduced in patients (Student's *t*-test, $p = 0.005$; Fig. 3C). Antibodies against the intracellular domain of Neurofascin exhibit cytoplasmic staining, representing the endosome-localized fraction of the protein [15]. A remarkable loss of Neurofascin was detected in neuronal cell bodies of patients, with less intense and more scattered staining (Fig. 3).

Immunoblotting neuronal lysates resulted in a single band at approximately 150 kDa and a significant reduction in the amount of Neurofascin protein (approximately to half of controls) in both patients compared to controls (Student's *t*-test, $p = 0.0058$; Fig. 4B–C).

Interestingly, immunoblotting Neurofascin in iPSC-derived neurons

resulted in a single band at ~150 kDa, which is the predicted size of the longest protein isoform in humans. However, in adult human nerve tissue, protein glycosylation of Neurofascin results in observed molecular weights of 186 kDa and 155 kDa (Fig. 4A), corresponding to the neuronal and glial isoforms respectively. This molecular weight discrepancy may be explained by a different pattern of glycosylation in cultured cells [16] or by the expression of an alternative *NFASC* splicing isoform in iPSC-derived neurons.

Subcellular fractionation of cultured neurons showed prevalent membrane localization of Neurofascin, as expected [17], and a strong reduction of the protein in the membrane of patient-derived cells compared to controls (Student's *t*-test, $p = 0.005$; Fig. 4D–E).

4. Discussion

We found a novel *NFASC* homozygous missense mutation in two siblings presenting with progressive infantile-onset ataxia with demyelinating neuropathy. The variant causes the substitution of a hydrophobic amino acid with a hydrophilic amino acid in the single transmembrane domain of the Neurofascin protein, suggesting a highly deleterious effect of the mutation. The functional studies described here are strongly consistent with *NFASC* being the most potential candidate gene, showing a significant reduction of the Neurofascin protein in iPSC-derived neurons from patients. However, a contribution of the splice variant of *NSMCE4A* remains plausible and requires further investigation.

Considering that the amount of *NFASC* mRNA is not decreased in patients' neurons, the reduction in Neurofascin is probably due to protein instability in membranes and accelerated turnover. Neurofascin is known to localize in the neuronal body, specifically at the level of the endo-lysosomal compartment. This would explain the punctate staining

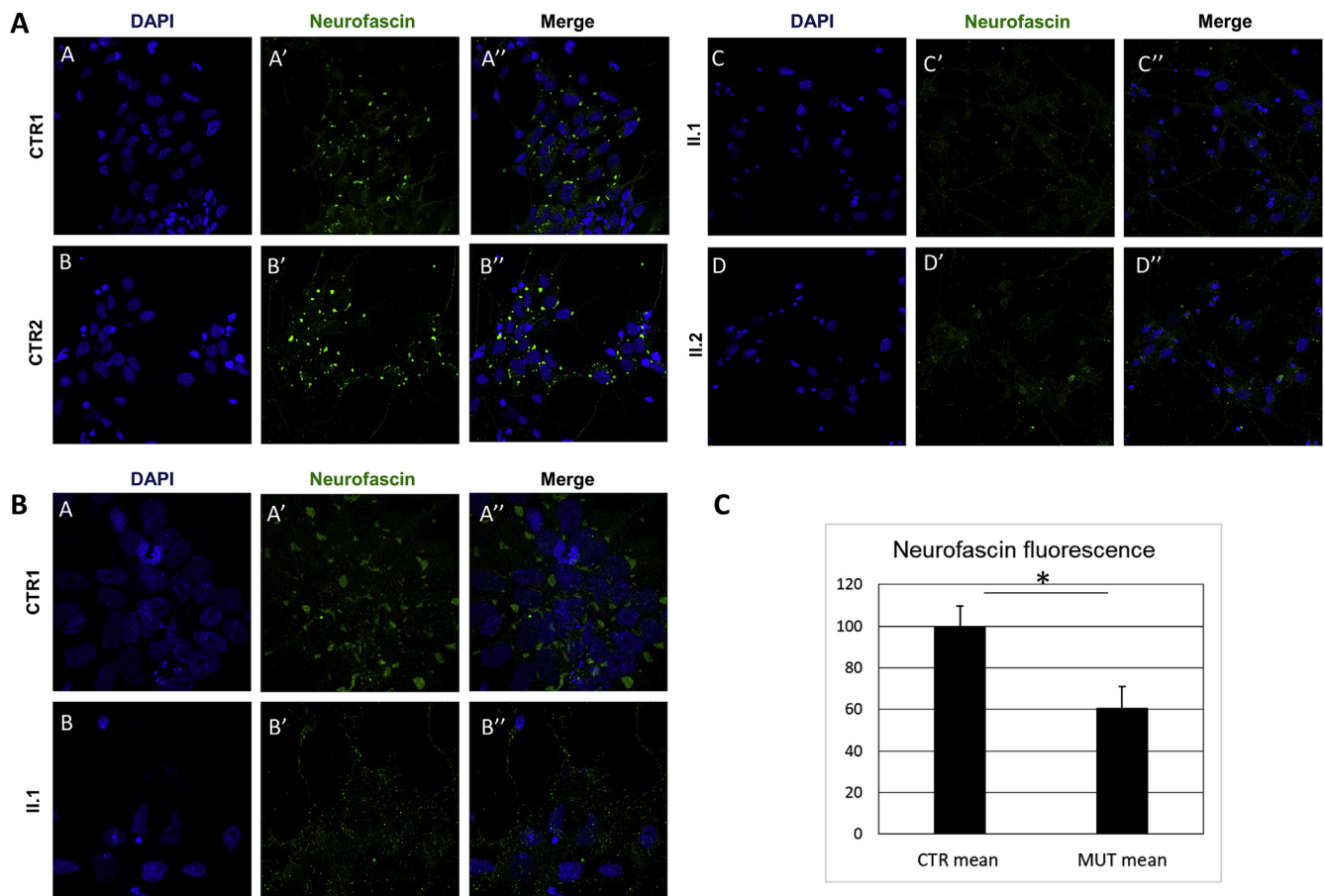


Fig. 3. ICF studies of iPSC-derived neurons. A–B) Skin biopsy-derived fibroblasts from the two affected siblings (II.1 and II.2) and three healthy controls (only CTR1 and CTR2 are shown) were reprogrammed into iPSCs and then differentiated into neurons. Confocal microscopy analysis showed discrete Neurofascin distribution (green) within control neuron somata and several spots of staining in neuronal extensions, whereas a remarkable loss and more scattered cytoplasmic staining of Neurofascin was detected in patients (bottom). 63x magnification (A) and 63 × 2 × -zoom magnification (B). C) Immunofluorescence quantification confirmed the statistically significant reduction of Neurofascin fluorescence in patients. * = $p < 0.01$. (For interpretation of the references to color in this figure legend, the reader is referred to the Web version of this article.)

in ICF analysis, which is strongly reduced and scattered in neurons from patients, in line with the significant reduction in Neurofascin on Western blot analysis.

Neurofascin plays an essential role in central and peripheral nervous system development and function; therefore, it is biologically plausible that dysfunction of this protein can cause a composite neurological disorder. Previously described *NFASC* knockout mouse models have been reported to have a neurological phenotype with important nodal and paranodal involvement. NF155-null mouse mutants exhibit severe ataxia, motor paresis, and reduced nerve conduction velocities, with a mean survival of approximately 3 weeks. In these mice, paranodal axoglial junctions fail to form, and myelinated axons undergo degeneration [18,19]. *NFASC* mutants lacking both the glial NF155 and neuronal NF186 died at post-natal day 6 and exhibited an extensive disruption of the nodal-paranodal region in the central and peripheral nervous systems, a strong reduction of nerve conduction velocities, and delayed/reduced myelination of the central nervous system [7,9].

Two *NFASC* homozygous mutations (NM_001160331.1: c.1109G > C: p.R370P and c.2536C > T: p.R846X) were recently proposed as the cause of a severe neurodevelopmental disorder in two families [20,21]. The disease presented a highly pleiotropic clinical phenotype, variably characterized by global developmental delay, hypertonia or hypotonia, neonatal respiratory distress, intellectual disability, areflexia, and facial dysmorphic features (hypertelorism, high and wide nasal bridge, micrognathia, glossoptosis, and cleft palate). Remarkably, brain MRI performed on one affected subject showed

diffuse white matter T2 hyperintensity [21].

Smigiel et al. [20] reported immunofluorescence staining of skin biopsies from the probands, revealing an absence of the NF155 isoform at the paranode of myelinated axons and the disruption of the nodal axoglial complex. Localization of the mutation in an exon present only in the transcript encoding NF155 explains the specific absence of the glial isoform.

The variable clinical phenotype may be caused by several factors: the severity of the mutation, the selective involvement of distinct Neurofascin isoforms by pathogenic variants, and the presence of genetic modifiers. In any case, the intra-familial and inter-familial phenotypic heterogeneity suggests a broad clinical spectrum associated with biallelic *NFASC* mutations. The description of additional cases is warranted in order to better define the *NFASC*-associated clinical phenotypes.

Neurofascin is well known to clinical neurologists because a significant proportion of chronic inflammatory demyelinating polyneuropathies (CIDPs) are caused by IgG4 antibodies against NF155 [22]. These cases are often associated with cerebellar ataxia and tremor [23]. Neuropathology on nerve biopsies shows minimal demyelination and a predominant injury to the nodes of Ranvier, which has prompted some authors to introduce the concept of nodopathy [24]. The nodes of Ranvier are ubiquitously present in myelinated structures of the central and peripheral nervous systems, including the cerebellum. The phenotypes associated with *NFASC* mutations clearly highlight the involvement of the central nervous system [20,21]. We propose expanding the

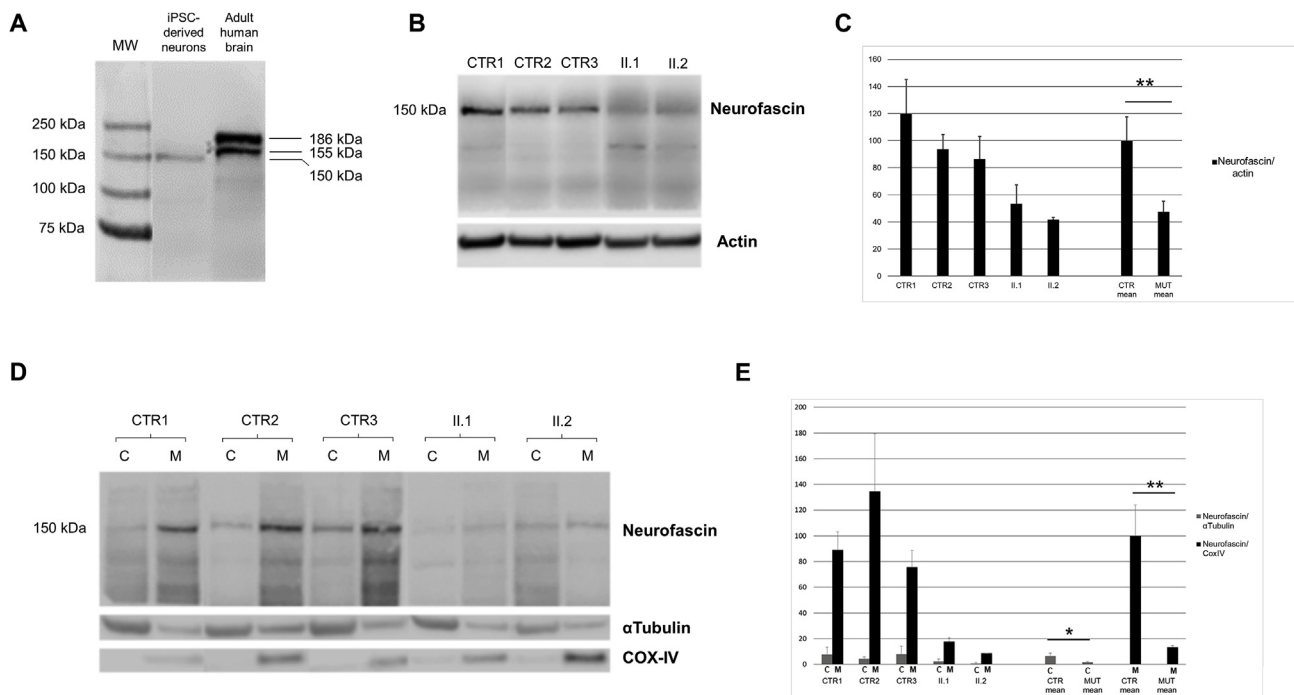


Fig. 4. Immunoblot studies of iPSC-derived neurons. A) Immunoblot with *anti*-Neurofascin antibody comparing iPSC-derived neurons with an adult human brain. In iPSC-derived neurons, there is a single band at ~150 kDa, different from the bands at 155 and 186 kDa in the adult human brain. B-C) Immunoblots of neuronal lysates demonstrate a single band at ~150 kDa and a significant reduction of Neurofascin protein (approximately to half of the controls) in both patients (II.1 and II.2) compared to controls (CTR1, CTR2, and CTR3). D-E) Subcellular fractionation of cultured neurons showed prevalent membrane localization of Neurofascin and a strong reduction of the protein in the membranes of patient-derived cells compared to controls ($p = 0.005$). α -Tubulin and COX-IV are cytosol and membrane-fraction markers respectively. M = membrane, C = cytosol, * = $p < 0.05$, ** = $p < 0.01$.

concept of nodopathy to central nervous system involvement, as there can be combined central and peripheral demyelination in *anti*-Neurofascin autoantibodies syndromes [22].

The neurophysiological results in the two affected siblings revealed slowing of the central and peripheral conduction velocities with more severe involvement of the central nervous system than the peripheral nervous system, and of motor fibers than sensory fibers, without conduction blocks, which are described as a common finding in acquired nodopathies [24]. The specific clinical neurophysiological features of patients with hereditary Neurofascin-related nodopathy could depend on the damaging potential of the causative mutation [25] and could be different from what is typically observed in acquired nodopathy [24], similarly to the differences commonly encountered between hereditary and acquired demyelinating polyneuropathies [26]. The issue of the neurophysiological spectrum of patients with genetic nodopathy should be addressed in future patients to better describe the pathophysiology and genotype-phenotype correlation.

In conclusion, the identification of *NFASC* as a causative gene for ataxia with demyelinating neuropathy paves the way for genetic research in the developing field of Neurofascin-related nodopathies of the central and peripheral nervous system.

Conflicts of interest

The authors report no competing interests.

Funding

This work was supported by funds from Fresco Institute for Parkinson's disease to ADF.

LS was supported by Fondazione Umberto Veronesi.

Acknowledgments

We thank all of the family members for their cooperation with this study.

Appendix A. Supplementary data

Supplementary data to this article can be found online at <https://doi.org/10.1016/j.parkreldis.2019.02.045>.

References

- [1] F. Ango, G. di Cristo, H. Higashiyama, V. Bennett, P. Wu, Z.J. Huang, Ankyrin-based subcellular gradient of neurofascin, an immunoglobulin family protein, directs GABAergic innervation at purkinje axon initial segment, *Cell* 119 (2) (2004) 257–272.
- [2] P.J. Thul, C. Lindskog, The human protein atlas: a spatial map of the human proteome, *Protein Sci.* 27 (1) (2018) 233–244.
- [3] L.J. Carithers, H.M. Moore, The genotype-tissue expression (GTEx) project, *Biopreserv. Biobanking* 13 (5) (2015) 307–308.
- [4] J.Q. Davis, S. Lambert, V. Bennett, Molecular composition of the node of Ranvier: identification of ankyrin-binding cell adhesion molecules neurofascin (mucin + /third FNIII domain-) and NrCAM at nodal axon segments, *J. Cell Biol.* 135 (5) (1996) 1355–1367.
- [5] E.D. Buttermore, C. Piochon, M.L. Wallace, B.D. Philpot, C. Hansel, M.A. Bhat, Pinceau organization in the cerebellum requires distinct functions of neurofascin in Purkinje and basket neurons during postnatal development, *J. Neurosci.* 32 (14) (2012) 4724–4742.
- [6] B. Zonta, A. Desmazieres, A. Rinaldi, S. Tait, D.L. Sherman, M.F. Nolan, P.J. Brophy, A critical role for Neurofascin in regulating action potential initiation through maintenance of the axon initial segment, *Neuron* 69 (5) (2011) 945–956.
- [7] B. Zonta, S. Tait, S. Melrose, H. Anderson, S. Harroch, J. Higginson, D.L. Sherman, P.J. Brophy, Glial and neuronal isoforms of Neurofascin have distinct roles in the assembly of nodes of Ranvier in the central nervous system, *J. Cell Biol.* 181 (7) (2008) 1169–1177.
- [8] I. Leshchynska, V. Sytnyk, Reciprocal interactions between cell adhesion molecules of the immunoglobulin superfamily and the cytoskeleton in neurons, *Front Cell Dev Biol* 4 (2016) 9.
- [9] D.L. Sherman, S. Tait, S. Melrose, R. Johnson, B. Zonta, F.A. Court, W.B. Macklin, S. Meek, A.J. Smith, D.F. Cottrell, P.J. Brophy, Neurofascins are required to

- establish axonal domains for saltatory conduction, *Neuron* 48 (5) (2005) 737–742.
- [10] M. Kriebel, J. Wuchter, S. Trinks, H. Volkmer, Neurofascin: a switch between neuronal plasticity and stability, *Int. J. Biochem. Cell Biol.* 44 (5) (2012) 694–697.
- [11] H. Li, R. Durbin, Fast and accurate short read alignment with Burrows-Wheeler transform, *Bioinformatics* 25 (14) (2009) 1754–1760.
- [12] A. McKenna, M. Hanna, E. Banks, A. Sivachenko, K. Cibulskis, A. Kernytsky, K. Garimella, D. Altshuler, S. Gabriel, M. Daly, M.A. DePristo, The Genome Analysis Toolkit: a MapReduce framework for analyzing next-generation DNA sequencing data, *Genome Res.* 20 (9) (2010) 1297–1303.
- [13] P. Zhang, N. Xia, R.A. Reijo Pera, Directed dopaminergic neuron differentiation from human pluripotent stem cells, *JoVE* 91 (2014) 51737.
- [14] C.A. Schneider, W.S. Rasband, K.W. Eliceiri, NIH Image to ImageJ: 25 years of image analysis, *Nat. Methods* 9 (7) (2012) 671–675.
- [15] C.C. Yap, M. Vakulenko, K. Kruczek, B. Motamedi, L. Digilio, J.S. Liu, B. Winckler, Doublecortin (DCX) mediates endocytosis of neurofascin independently of microtubule binding, *J. Neurosci.* 32 (22) (2012) 7439–7453.
- [16] P. Hossler, S.F. Khattak, Z.J. Li, Optimal and consistent protein glycosylation in mammalian cell culture, *Glycobiology* 19 (9) (2009) 936–949.
- [17] F.G. Rathjen, J.M. Wolff, S. Chang, F. Bonhoeffer, J.A. Raper, Neurofascin: a novel chick cell-surface glycoprotein involved in neurite-neurite interactions, *Cell* 51 (5) (1987) 841–849.
- [18] C. Thaxton, A.M. Pillai, A.L. Pribisko, M. Labasque, J.L. Dupree, C. Faivre-Sarrailh, M.A. Bhat, In vivo deletion of immunoglobulin domains 5 and 6 in neurofascin (Nfasc) reveals domain-specific requirements in myelinated axons, *J. Neurosci.* 30 (14) (2010) 4868–4876.
- [19] A.M. Pillai, C. Thaxton, A.L. Pribisko, J.G. Cheng, J.L. Dupree, M.A. Bhat, Spatiotemporal ablation of myelinating glia-specific neurofascin (Nfasc NF155) in mice reveals gradual loss of paranodal axoglial junctions and concomitant disorganization of axonal domains, *J. Neurosci. Res.* 87 (8) (2009) 1773–1793.
- [20] R. Smigiel, D.L. Sherman, M. Rydzanicz, A. Walczak, P. Mikolajkow, B. Krolak-Olejnik, J. Kosinska, P. Gasperowicz, A. Biernacka, P. Stawinski, M. Marciniak, W. Andrzejewski, M. Boczar, P. Krajewski, M.M. Sasiadek, P.J. Brophy, R. Ploski, Homozygous mutation in the Neurofascin gene affecting the glial isoform of Neurofascin causes severe neurodevelopment disorder with hypotonia, amimia and areflexia, *Hum. Mol. Genet.* 27 (21) (2018) 3669–3674.
- [21] S. Anazi, S. Maddirevula, V. Salpietro, Y.T. Asi, S. Alsahli, A. Alhashem, H.E. Shamseldin, F. AlZahrani, N. Patel, N. Ibrahim, F.M. Abdulwahab, M. Hashem, N. Alhashmi, F. Al Murshedi, A. Al Kindy, A. Alshaer, A. Rumayyan, S. Al Tala, W. Kurdi, A. Alsaman, A. Alasmari, S. Banu, T. Sultan, M.M. Saleh, H. Alkuraya, M.A. Salih, H. Aldhalaan, T. Ben-Omran, F. Al Musafri, R. Ali, J. Suleiman, B. Tabarki, A.W. El-Hattab, C. Bupp, M. Alfadhel, N. Al Tassan, D. Monies, S.T. Arold, M. Abouelhoda, T. Lashley, H. Houlden, E. Faqeih, F.S. Alkuraya, Expanding the genetic heterogeneity of intellectual disability, *Hum. Genet.* 136 (11–12) (2017) 1419–1429.
- [22] N. Kawamura, R. Yamasaki, T. Yonekawa, T. Matsushita, S. Kusunoki, S. Nagayama, Y. Fukuda, H. Ogata, D. Matsuse, H. Murai, J. Kira, Anti-neurofascin antibody in patients with combined central and peripheral demyelination, *Neurology* 81 (8) (2013) 714–722.
- [23] J.J. Devaux, Y. Miura, Y. Fukami, T. Inoue, C. Manso, M. Belghazi, K. Sekiguchi, N. Kokubun, H. Ichikawa, A.H. Wong, N. Yuki, Neurofascin-155 IgG4 in chronic inflammatory demyelinating polyneuropathy, *Neurology* 86 (9) (2016) 800–807.
- [24] A. Uncini, S. Kuwabara, Nodopathies of the peripheral nerve: an emerging concept, *J. Neurol. Neurosurg. Psychiatry* 86 (11) (2015) 1186–1195.
- [25] Robert Smigiel, Diane L. Sherman, Małgorzata Rydzanicz, Anna Walczak, Dorota Mikolajkow, Barbara Krolak-Olejnik, Joanna Kosinska, Piotr Gasperowicz, Anna Biernacka, Piotr Stawinski, Malgorzata Marciniak, Witalij Andrzejewski, Maria Boczar, Pawel Krajewski, Maria M. Sasiadek, Peter J. Brophy, Rafal Ploski, Homozygous mutation in the Neurofascin gene affecting the glial isoform of Neurofascin causes severe neurodevelopment disorder with hypotonia, amimia and areflexia, *Hum. Mol. Genet.* 27 (21) (1 November 2018) 3669–3674 <https://doi.org/10.1093/hmg/ddy277>.
- [26] D. Pareyson, V. Scaiola, M. Laura, Clinical and electrophysiological aspects of Charcot-Marie-Tooth disease, *NeuroMolecular Med.* 8 (1–2) (2006) 3–22.
- [27] H. McWilliam, W. Li, M. Uludag, S. Squizzato, Y.M. Park, N. Buso, A.P. Cowley, R. Lopez, Analysis tool web services from the EMBL-EBI, *Nucleic Acids Res.* 41 (2013) W597–W600 Web Server issue.